

AD-A055 746

NORTHWESTERN UNIV EVANSTON ILL DEPT OF PHYSICS  
ELECTRONICALLY DRIVEN PHONON ANOMALIES AND PHASE TRANSFORMATION--ETC(U)  
MAY 78 A J FREEMAN, M GUPTA, H W MYRON

F/6 20/12

AFOSR-76-2948

UNCLASSIFIED

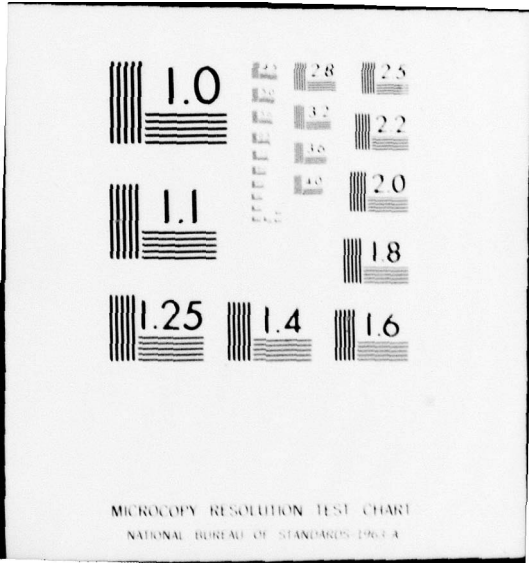
AFOSR-TR-78-1018

NL

| OF |  
AD  
A055 746



END  
DATE  
FILMED  
8 -78  
DDC



MICROCOPY RESOLUTION TEST CHART  
NATIONAL BUREAU OF STANDARDS-1963-A

2

Unclassified  
SECURITY CLASSIFICATION OF THIS PAGE (When Data Entered)

AD A 055746

18. REPORT DOCUMENTATION PAGE		READ INSTRUCTIONS BEFORE COMPLETING FORM	
1. REPORT NUMBER AFOSR/TR-78-1013		3. RECIPIENT'S CATALOG NUMBER	
2. GOVT ACCESSION NO.		4. TITLE (and Subtitle) Electronically Driven Phonon Anomalies and Phase Transformations	
5. AUTHOR(s) A. J./Freeman, M./Gupta H.W./Myron, J./Rath T.J./ Waston-Yang		6. TYPE OF REPORT & PERIOD COVERED Interim rept.	
7. PERFORMING ORGANIZATION NAME AND ADDRESS Northwestern University Dept. of Physics and Astronomy Evanston, Illinois 60201		8. CONTRACT OR GRANT NUMBER(s) AFOSR-76-2948, NSF-DMR 72- 103101	
9. CONTROLLING OFFICE NAME AND ADDRESS AFOSR/NP Bolling AFB, Bldg. 410 Washington, D. C. 20332		10. PROGRAM ELEMENT, PROJECT, TASK AREA & WORK UNIT NUMBERS 61102F 9767-04	
11. MONITORING AGENCY NAME & ADDRESS (if different from Controlling Office)		12. NUMBER OF PAGES 8	
12. DISTRIBUTION STATEMENT (of this Report) Approved for public release; distribution unlimited		13. SECURITY CLASS. (of this report) Unclassified	
13. DISTRIBUTION STATEMENT (of the abstract entered in Block 20, if different from Report)		14. DECLASSIFICATION/DOWNGRADING SCHEDULE	
14. SUPPLEMENTARY NOTES Proc. of Conf. on Lattice Dynamics, Paris, 1977 p204-210 1978			
15. KEY WORDS (Continue on reverse side if necessary and identify by block number)			
16. ABSTRACT (Continue on reverse side if necessary and identify by block number) See reverse side			

AU NO. DDC FILE COPY

A034092  
372

78 06 19 078

402 694

Dur

We have studied the possible role of electronic structure on observed phonon anomalies and phase transformations by means of accurate calculations of the generalized response function,  $\chi(\vec{q})$ , for non-interacting conduction electrons. Both Fermi surface "nesting" (parallel sections of Fermi surface) and so-called "volume" effects (parallel electron-hole bands crossing the  $E_F$ ) are included using results of energy band calculations and our recently developed analytic tetrahedron linear energy method. Correlations of the positions of phonon anomalies and/or the occurrence of phase transformations with large maxima in  $\chi(\vec{q})$  are found and provide strong evidence that they arise from an electronically driven divergence in  $\chi(\vec{q})$ : (1) In 1T-TaS<sub>2</sub> and 1T-TaSe<sub>2</sub>, large peaks in  $\chi(\vec{q})$  are found at the observed  $q$  values along  $\Gamma M$  corresponding to the CDW. (2) In both Pd and Pt metals, a large peak is found at precisely that  $q$  value along [110] for which large Kohn anomalies have been found. An additional peak is found along [111] which predicts the occurrence of a Kohn anomaly in this direction (but which is stronger in Pd than in Pt). (3) Large peaks in  $\chi(\vec{q})$  are found for both NbC and TaC at precisely those  $q$  values at which soft modes were observed by Smith and Glaser. Maxima in  $\chi(\vec{q})$  are predicted for other directions. The locus of these  $q_{max}$  values can be represented by a warped cube of dimension  $\sim 1.2 (2\pi/a)$  in momentum space - in striking agreement with the soft mode surface proposed phenomenologically by Weber. No such peaks are found for ZrC and HfC, for which no phonon anomalies have been observed. (4) For the tetragonal rutile phase of VO<sub>2</sub>, we find a large maximum in  $\chi(\vec{q})$  at the zone boundary R. This suggests the possible formation of a CDW with  $q=\Gamma R$ . The subsequent condensation of phonons at R could then explain the crystallographic (metal to semiconducting) phase transition at T=340. Recent x-ray diffuse scattering measurements by Terauchi and Cohen of Northwestern confirm these predictions; their results show a lattice instability near the metal-insulator transition to occur at the R point.

85530A  
 402238

ACCESSION for		
NTIS	White Section	<input checked="" type="checkbox"/>
DOC	Buff Section	<input type="checkbox"/>
UNANNOUNCED		<input type="checkbox"/>
JUSTIFICATION.....		
BY.....		
DISTRIBUTION/AVAILABILITY CODES		
Dist.	AVAIL. and/or SPECIAL	
A	<del>SECRET</del>	

## ELECTRONICALLY DRIVEN PHONON ANOMALIES AND PHASE TRANSFORMATIONS \*

A.J. Freeman

Department of physics and Astronomy and Materials Research Center,  
Northwestern University, Evanston, Illinois 60201, U.S.A., and  
Argonne National Laboratory, Argonne, Illinois 60439, U.S.A.,

and

M. Gupta, H.W. Myron<sup>†</sup>, J. Rath<sup>††</sup>, and T.J. Waston-Yang,  
Department of Physics and Astronomy, Northwestern University,  
Evanston, Illinois 60201, U.S.A.

We have studied the possible role of electronic structure on observed phonon anomalies and phase transformations by means of accurate calculations of the generalized response function,  $\chi(\vec{q})$ , for non-interacting conduction electrons. Both Fermi surface "nesting" (parallel sections of Fermi surface) and so-called "volume" effects (parallel electron-hole bands crossing the  $E_F$ ) are included using results of energy band calculations and our recently developed analytic tetrahedron linear energy method. Correlations of the positions of phonon anomalies and/or the occurrence of phase transformations with large maxima in  $\chi(\vec{q})$  are found and provide strong evidence that they arise from an electronically driven divergence in  $\chi(\vec{q})$ : (1) In 1T-TaS<sub>2</sub> and 1T-TaSe<sub>2</sub>, large peaks in  $\chi(\vec{q})$  are found at the observed  $q$  values along  $\Gamma M$  corresponding to the CDW. (2) In both Pd and Pt metals, a large peak is found at precisely that  $q$  value along [110] for which large Kohn anomalies have been found. An additional peak is found along [111] which predicts the occurrence of a Kohn anomaly in this direction (but which is stronger in Pd than in Pt). (3) Large peaks in  $\chi(\vec{q})$  are found for both NbC and TaC at precisely those  $q$  values at which soft modes were observed by Smith and Glaser. Maxima in  $\chi(\vec{q})$  are predicted for other directions. The locus of these  $q_{\max}$  values can be represented by a warped cube of dimension  $\sim 1.2 (2\pi/a)$  in momentum space - in striking agreement with the soft mode surface proposed phenomenologically by Weber. No such peaks are found for ZrC and HfC, for which no phonon anomalies have been observed. (4) For the tetragonal rutile phase of VO<sub>2</sub>, we find a large maximum in  $\chi(\vec{q})$  at the zone boundary R. This suggests the possible formation of a CDW with  $q=\Gamma R$ . The subsequent condensation of phonons at R could then explain the crystallographic (metal to semiconducting) phase transition at  $T=340$ . Recent x-ray diffuse scattering measurements by Terauchi and Cohen of Northwestern confirm these predictions; their results show a lattice instability near the metal-insulator transition to occur at the R point.

## 1. INTRODUCTION

Recent theoretical and experimental developments have called attention to the central role played by the generalized susceptibility function  $\chi(\vec{q})$  in the understanding of many physical phenomena in solids. Since  $\chi(\vec{q})$  measures the response of the system to an external (generally spatially in-

homogeneous) perturbation, emphasis has been placed on possible anomalous behaviour which may result from an instability in the conduction electron gas as a result of a divergence in this response function. In linear-response theory

$$\chi(\vec{q}) = \chi(\vec{q}) / (1 - I(\vec{q})\chi(\vec{q})) \quad (1)$$

where  $I(\vec{q})$  is the electron-electron inter-

\* Supported by the Air Force Office of Scientific Research, the National Science Foundation (DMR Grant Nos DMR-72-03101-A02 and DMR 72-03019) and the United States Energy Research and Development Administration. ~~AFOSR-76-2948~~

<sup>†</sup> Present address : Nijmegen University, Dept. of Physics, Nijmegen, The Netherlands.

<sup>††</sup> Present address : University of Missouri, Dept. of Physics, Columbia, Missouri 65201.

action and  $\chi(\vec{q})$  is the bare susceptibility defined as

$$\chi(\vec{q}) = \sum_{n, n', \vec{k}} \frac{|M_{n, n'}^{\vec{k}, \vec{k}+\vec{q}}|^2 f_{n, \vec{k}} (1 - f_{n', \vec{k}+\vec{q}})}{E_{n', \vec{k}+\vec{q}} - E_{n, \vec{k}}} \quad (2)$$

for bands  $n$  and  $n'$  and wavevector  $\vec{k}$ . The  $f$ 's are the Fermi occupation numbers for occupied and empty states and the  $M$ 's denote oscillator strength matrix elements.

Since the early work of Overhauser, attention has been drawn to the role of Fermi surface "nesting" features, i.e. the existence of large parallel pieces of Fermi surface, in leading to a divergence in  $\chi(\vec{q})$  and possibly to a divergence in  $\chi(\vec{q})$  itself, depending on the value of  $I(\vec{q})$ . More recently, the possible role of so-called "volume" effects (parallel electron-hole bands crossing the Fermi energy) in producing divergences in  $\chi(\vec{q})$  has been emphasized. The physical mechanism leading to either a spin density wave (SDW) or charge density wave (CDW) state is that a lower energy state results from the promotion of electrons from orbitals of one spin to orbitals of the same (or opposite) spin sustained by the Fermi surface, or band, geometry favourable to electron-hole excitations. Such a repopulation can also be achieved by the scattering of the electrons by phonons through the electron-phonon interaction. It can be shown that  $\chi(\vec{q})$  plays an important role in the expression of renormalized phonon frequencies and that, under simplifying assumptions, a divergence in  $\chi(\vec{q})$  can lead to a softening of the corresponding vibrational mode.

In this paper, we focus the physical information contained in the generalized susceptibility function alone and indicate the sort of understanding presently available from accurate calculations of  $\chi(\vec{q})$  based on accurate first principles band structure calculations. As examples, taken from the work of our group, we cite correlations of peaks in  $\chi(\vec{q})$  with observed CDW's in 1T-TaS<sub>2</sub> and TaSe<sub>2</sub>, phonon anomalies<sup>2</sup> in transition metal carbides, phonon anomalies<sup>3</sup> in Pd and Pt and the origin of the metal-insulator transition<sup>4</sup> in the classic case of VO<sub>2</sub>. Although neglected in what follows, we emphasize that electronic Coulomb exchange and correlation interactions, as well as the electron-phonon matrix elements play a major role in producing the observed anomalies. This makes it all the more remarkable that the bare susceptibility response function calculated from the band structure alone has been successful in predicting these phenomena.

## 2. METHODOLOGY

There are two steps required for the accurate determination of  $\chi(\vec{q})$  in the constant matrix elements approximation: (1) the accurate determination of the underlying electronic band structure and (2) a highly precise method for carrying out the phase-space (Brillouin zone) integral (summation)

of a spectral Green's function (Eq.2). The energy band method is now well accepted for successfully providing accurate eigenvalues and hence energy related results in quite good agreement with experiment including complex metals and compounds. We report results based on the KKR (Green's function) method<sup>1</sup>, the non-relativistic and relativistic APW methods<sup>2,3</sup> and the analytic LCAO basis set Discrete Variational Method (DVM). For the precise calculations of  $\chi(\vec{q})$  we use the analytic tetrahedron linear energy method<sup>4</sup> which we have derived as an extension of the work of Jepsen and Andersen<sup>5</sup> and Lehmann et al.<sup>7</sup> on the density of states problem. In this method, using tetrahedrons as microzones with which to divide the BZ, a geometrical analysis is made of the occupied and unoccupied regions of any tetrahedron which reduces the problem of calculating  $\chi(\vec{q})$  essentially to the problem of performing a volume integral over a tetrahedron with a linearized energy denominator. This procedure yields simple analytic expressions for the BZ integral which depend only on the volume of the tetrahedron and the differences of energies,  $\Delta E_n(\vec{k})$ , at its corners. The result is a computational scheme - not limited to constant matrix elements - which is highly accurate and, because of its simplicity, rapid to perform.

## 3. APPLICATIONS - CHARGE DENSITY WAVES IN 1T-TaS<sub>2</sub> AND 1T-TaSe<sub>2</sub>

In one of our earliest investigations, we reported results of detailed *ab initio* studies of  $\chi(\vec{q})$  for the 1T polymorphs of both TaS<sub>2</sub> and TaSe<sub>2</sub>; these systems were of great interest because of the existence, revealed by electron diffraction studies<sup>8,9</sup>, of CDW's and their accompanying periodic lattice distortions. The band structures were determined by the KKR method. The Fermi surfaces (FS) of both metals were found to be very similar, having cross sections which are approximately constant in planes that are perpendicular to the  $z$  axis and which can be nested by approximately the same wavevector parallel to the  $\Gamma M$  direction<sup>1</sup>. In this regard, it is important to emphasize that our FS are quite different from the one derived from Mattheiss' limited number of  $k$  points result<sup>10</sup> by Wilson and associates<sup>8</sup>. This incorrect FS yields dominant nesting along the  $\Gamma K$  direction which agreed with the first (erroneous) report of the direction of the CDW  $\vec{q}$  vector but not the second (correct) report<sup>8</sup> of  $\vec{q}$  along the  $\Gamma M$  direction. We also showed that the response function,  $\chi(\vec{q})$ , contained not only information about the FS features (i.e. nesting) but also about band structure effects for states just above and below the Fermi energy (volume effects). Both effects were found to contribute substantially to the important structure found in  $\chi(\vec{q})$ . These accurate calculations showed major peaks to occur in the case of TaSe<sub>2</sub>, at the  $\vec{q}$  value corresponding to the observed CDW vectors. For TaSe<sub>2</sub>, which

shows two anomalies in the resistivity with temperature (whereas TaSe<sub>2</sub> shows only one), we find two peaks in  $\chi(\vec{q})$  along the FM direction. Although a direct connection is perhaps somewhat tenuous, it is striking that this feature in  $\chi(\vec{q})$  may well relate to the observed resistivity anomalies. The interested reader is referred to the original paper for details and a fuller discussion which appears to provide a detailed confirmation of the role of electronically driven instabilities as the origin of the observed CDW in these metals.

Most recently, Zunger and Freeman<sup>11</sup> have studied  $\Gamma$ -TiSe<sub>2</sub> by means of accurate numerical basis set LCAO-DVM calculations. They find that this material is a semi-metal - unlike TiS<sub>2</sub> which is an indirect gap semiconductor - with hole pockets at  $\Gamma$  and electron pockets at L. The band structure and Fermi surface thus allow for the electron-hole coupling which leads to the formation of the  $2a_0 \times 2c_0$  superlattice phase. These results are utilized and a FS construction based on the Zunger-Freeman work is presented at this meeting. The interested reader is referred to that paper for further details.

#### PHONON ANOMALIES IN TRANSITION METAL CARBIDES

Interest in the transition metal carbides (TMC) - always high because of their remarkable physical properties - reached a peak because of the finding of strong phonon softening<sup>12</sup> and high superconducting transition temperatures. Thus, it became very important to understand the origin of phonon anomalies in these systems.

Here, we wish to call attention to the predictions of the occurrence of soft phonon modes obtained from ab initio (model independent band) calculations<sup>2</sup> of  $\chi(\vec{q})$ , again in the constant matrix element approximation. Since results have been presented in detail elsewhere, we provide only a summary here for purposes of discussion and comparison with the models discussed in the following papers.

The ab initio band structures of NbC and TaC were determined using the APW method and a warped muffin tin form of potential (spherically symmetric inside the APW spheres and full - i.e., non-constant-potential between spheres). Convergence was obtained to within 1 mRy in the energy eigenvalues obtained at 89 points in the  $1/48$  irreducible BZ. The band structures for both compounds were found to be very similar and to yield very similar Fermi surfaces. The Fermi energy,  $E_F$ , was found, in both compounds, to fall at a very low value of the density of states. The band structure eigenvalues were fitted by an expansion into a set of 50 symmetrized plane waves and used in the determination of  $\chi(\vec{q})$ .

The remarkable result of these calculations is the existence of strong structure in the contribution from band 4 to  $\chi(\vec{q})$ . More specifically, the maxima in  $\chi(\vec{q})$ , which occur

at  $\vec{q} = (0.6, 0.0, 0.0)$ ;  $\vec{q} = (0.55, 0.55, 0.0)$ ,  $\vec{q} = (0.5, 0.5, 0.5)$  in  $2\pi/a$  units for NbC match exactly with the positions of the dips in the longitudinal acoustic branches of the measured<sup>12</sup> dispersion curves in the [100], [110], and [111] symmetry directions. For TaC, the position of the maxima in the calculated  $\chi(\vec{q})$  band-4 contribution found at  $\vec{q} = (0.63, 0.0, 0.0)$ ,  $\vec{q} = (0.55, 0.55, 0.0)$ , and  $\vec{q} = (0.5, 0.5, 0.5)$ , are also in excellent agreement with experiment for the [110] and [111] directions. Even more remarkable, in the [100] direction, the small shift in the  $\vec{q}$  value at which the anomaly occurs in going from NbC to TaC ( $q_{th}=0.60$  vs  $0.63$ ) reproduces the trend in the shift observed experimentally ( $q_{exp}=0.60$  vs  $0.65$ ).

We must also emphasize the large magnitude of the calculated maxima in  $\chi(\vec{q})$ . For band 4, the peaks in [100], [110], and [111] directions show an increase of 33.3%, 55.2%, 91.7% for NbC and an increase of 32%, 53%, 90% for TaC from the value of the function at  $q=0$  (which is the contribution from band 4 to the DOS at  $E_F$ ). A striking feature of these results is that the ratios of these maxima also match closely to the magnitude of the depth of the mode softening - as can be seen by calculating  $\omega^2(\text{ZrC}) - \omega^2(\text{NbC})$  or  $\omega^2(\text{HfC}) - \omega^2(\text{TaC})$  at those  $q$  values where anomalies occur for NbC or TaC (note that ZrC and HfC do not possess any phonon anomalies). The calculated peaks are broad, as are the dips observed in the dispersion curves. We also studied an arbitrary off-symmetry direction  $\Gamma$  to W defined by  $(\xi, \xi/2, 0)$  with  $0 \ll \xi \ll 2$ . Our results show that the  $\chi_4(\vec{q})$  function has a maximum at  $\xi \sim 0.65$  for NbC and TaC in the  $\Gamma$ -W directions. Taken together, our calculations show that the maxima of  $\chi_4(\vec{q})$  lie on the surface of a warped cube in  $q$  space, centered at  $\Gamma$  and of approximate dimension  $\sim 1.2$  ( $2\pi/a$ ). This result is in striking agreement with the soft mode surface proposed by Weber<sup>13</sup> starting from an entirely different (and phenomenological) formulation.

As a further test of the role played by structure in  $\chi(\vec{q})$  in the occurrence of phonon anomalies, we calculated  $\chi(\vec{q})$  for the 8 valence-electron compounds ZrC and HfC, by applying the rigid-band model to the NbC and TaC energy band results, respectively. Unlike the case of NbC and TaC, we find for ZrC and HfC that both the individual and the total interband contributions to  $\chi(\vec{q})$  decrease in all directions from the value at  $\chi(\vec{q})=0$ . This results in a maximum at  $\Gamma$  and, consequently, in an overscreening at the zone center. These results correlate very well with the experimental results<sup>12</sup> where the optic modes at  $\Gamma$  in ZrC and HfC have a significantly lower value than in NbC and TaC; the decrease at  $\Gamma$  is from  $\sim 17$  to  $\sim 13$  THz from NbC to ZrC. The general decrease of  $\chi(\vec{q})$  away from  $\Gamma$  is also consistent with the fact that no anomalies are present in this low  $T_C$  compound. We thus conclude from this study of the 9 and 8 valence-electrons TMC that the phonon anomalies of these com-

pounds can be explained essentially as being due to an anomalous increase in the response function of the conduction electrons, resulting in a strong screening of the corresponding phonon modes.

#### PHONON ANOMALIES IN Pd AND Pt METALS

In their classic paper, Miller and Brockhouse<sup>14</sup> observed an anomaly in the slope of the  $[0\bar{1}\bar{1}]$   $T_1$  branch of the dispersion curves for palladium. The anomaly not only extended over a broad range of wavevector space but also decreased rapidly in amplitude with increasing temperature. Later, Dutton et al.<sup>15</sup> also found a rather similar but not identical anomaly in the  $T_1$  branch of platinum. On the basis of the known Fermi surfaces, these anomalies were suggested<sup>16</sup> as arising from the generalized Kohn effect due to nesting.

We have studied the possible occurrence of generalized Kohn anomalies by direct calculation of the generalized susceptibility,  $\chi(\vec{q})$ . We find that a peak in  $\chi(\vec{q})$  can be directly related to the observed anomaly in the  $[0\bar{1}\bar{1}]$   $T_1$  branch of the dispersion curves of Pt and Pd.

We calculated the band structure for Pd<sup>17</sup> using the APW method and the relativistic APW scheme for Pt<sup>18</sup> - both with a warped muffin tin potential. The band structures were previously found<sup>17,18</sup> to yield Fermi surface radii, temperature dependencies of the static magnetic susceptibility,  $\chi(T)$ , resistivity, and a spin lattice relaxation,  $T_1T$ , in very good agreement with experiment.

In the  $\chi(\vec{q})$  calculations<sup>19</sup>, we used 2048 tetrahedra in  $1/48$ 'th irreducible BZ and the energy eigenvalues as fitted to a Fourier series representation. The results of  $\chi(\vec{q})$  for  $\vec{q}$  along  $[010]$ ,  $[110]$  and  $[111]$  directions were calculated for Pd and for Pt for bands 4, 5 and 6 which cross the Fermi energy. The intraband parts of  $\chi(\vec{q})$  at  $\vec{q}=0$  for both metals are found to agree with the density of states at the Fermi energy to within 0.5%. Results show that the dominant contribution to  $\chi_{\text{intra}}$  arise from the dominant band 5 whose "jungle-gym" FS has strong nesting features; the main peak for Pd occurs at the same  $\vec{q}$  value ( $=0.65 \pi/a$ ) for  $\vec{q}$  along the  $[0q0]$ ,  $[qq0]$  and  $[qqq]$  directions. The locus of this main peak is a square in the  $(0,0,1)$  plane. The maximum of  $\chi_{\text{intra}}$  for  $\vec{q}$  along the  $[110]$  and  $[111]$  directions are 23% and 12% respectively higher than the value of  $\chi(\vec{q})$  at  $\vec{q}=0$ . For  $\vec{q}$  along the  $[010]$  direction, the peak is, however, 5.4% lower than the value of  $\chi_{\text{intra}}$  at  $\vec{q}=0$ . Hence, while phonon anomalies are predicted for the  $[110]$  and  $[111]$  directions, no anomaly is predicted for the  $[100]$  direction. The predicted  $\vec{q}$  value for the  $[110]$  anomaly,  $q=0.65 \pi/a$  is close to the experimental value of  $\sim 0.7 \pi/a$ . Although there may be a hint of an anomaly at  $0.56 [111]$  in the measurements, a more detailed investigation of this region is called for.

For platinum,  $\chi_{\text{intra}}$  for  $\vec{q}$  along the

$[010]$ ,  $[110]$  and  $[111]$  directions has main peaks which occur at  $\vec{q}=0.68 \pi/a$ ,  $0.75 \pi/a$ , and  $0.85 \pi/a$ , respectively. Here too, this main peak comes from the nesting of the jungle-gym Fermi surface which is not, however, as flat as that of palladium. Anomalies are predicted (although weaker than in Pd) along  $[110]$  and  $[111]$  but not at  $[100]$ . The  $[110]$  anomaly is close to the measured  $\vec{q}$  value ( $\sim 0.7-0.8 \pi/a$ ). Also in agreement with experiment, we predict a weaker  $[110]$  anomaly for Pt than for Pd, i.e. the ratio of  $[\chi_{\text{intra}}(q_{\text{max}}) - \chi_{\text{intra}}(q=0)]$  to  $\chi_{\text{intra}}(q=0)$  is 23% for Pd versus 12% for Pt. In both Pd and Pt, weaker anomalies are predicted for the  $[111]$  direction than for the  $[110]$  direction.

We have also calculated  $\chi(\vec{q})$  of both Pd and Pt for  $\vec{q}$  along an off-symmetry direction,  $\Gamma W$ . These results also show peaks from band 5 which arise from nesting FS features but which are lower than  $\chi(q=0)$ . These results are consistent with Miller's observations for the "off-symmetry" direction in the  $(001)$  plane making an angle  $\theta=30^\circ$  and is no longer visible at  $\theta=45^\circ$ .

#### LATTICE INSTABILITY AND METAL-INSULATOR TRANSITION IN $\text{VO}_2$

The classic case of a metal-insulator transition occurs in  $\text{VO}_2$  at 340K. The crystallographic phase transformation from monoclinic rutile to the tetragonal rutile structure is accompanied by an abrupt jump in metallic conductivity ( $\sim 10^5$ ) and a jump in magnetic susceptibility.  $\text{VO}_2$  does not order magnetically at low temperatures. We have investigated<sup>4</sup> whether the electronic properties, e.g., Fermi surface geometry and response function of the system, can account for the possible formation of a charge density wave (CDW) which could lead, through the electron-phonon coupling, to the renormalization of a phonon frequency, the corresponding phonon mode becoming overdamped at  $T=T_C$ , and driving the lattice to a new structural phase. This mechanism of a structural phase transformation proceeding via a soft phonon mode is well known in other materials.

We have performed a first principles energy band study of the metallic rutile phase of  $\text{VO}_2$ , using a general crystal potential and an expansion of the Bloch functions in a linear combination of atomic orbitals. We obtained a large density of states at the Fermi energy. The Fermi surface is found to be determined by the two lowest d bands, at the bottom of the " $t_{2g}$ " manifold which is split by the orthorhombic field; the lowest band Fermi surface possesses nesting features corresponding to a nesting vector  $\vec{q}=\Gamma R$  (see Fig.1).

We here focus on the physical information contained in the generalized susceptibility function alone. The intra-band contribution from bands 1 and 2 and the total interband contributions from the 6 bands belonging to the  $t_{2g}$  manifold are plotted

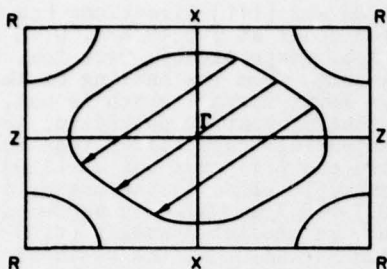


Fig. 1 Fermi surface cross-section of band 1 in the  $\Gamma$ ZR plane. Dotted portions indicate occupied regions; arrows indicate the nesting  $\vec{q}=\Gamma R$ .

separately in Fig. 2, along 3 high symmetry directions  $R(1,0,1)$ ,  $P(1/2,1/2,1)$  and  $RP(\xi,1/2-\xi,1/2)$ . The total intraband value increases away from  $\Gamma$  and shows a sharp rise at the zone boundary R. The peak at R in the intraband function corresponds to a 29% in-

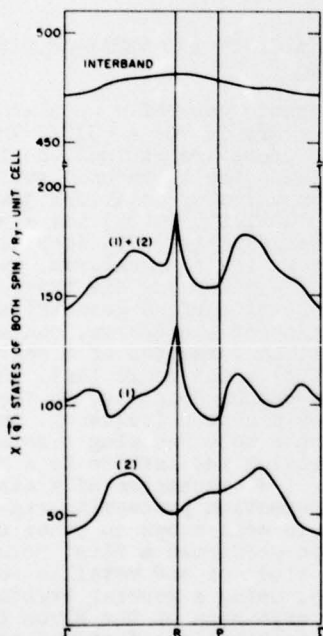


Fig. 2 The generalized susceptibility function  $\chi(\vec{q})$  of metallic  $VO_2$  is given along several symmetry directions, with contributions from the lowest six "V 3d" conduction bands. Curve (1) is the intraband contribution of band 1; curve (2) the intraband contribution of band 2; the curve labelled (1)+(2) is the total intraband contribution. The upper curve is the sum of all interband contributions from the six bands belonging to the fully split " $t_{2g}$ " manifold; note the break in the vertical scale.

crease from the value at  $\Gamma$ ; this peak is due to the band 1 contribution and can be associated with the "nesting" features with wavevector  $\vec{q}=(1/2,0,1/2)$  mentioned above. The magnitude of band 1 contribution to  $\chi(\vec{q})$  is generally 50% higher than the band 2 contribution throughout the Brillouin zone. This latter contribution shows in the  $\Gamma R$  direction a broad structure for  $0.3 < q < 0.8$  associated with contributions from the FS piece around  $\Gamma$ , as the electron pocket around R has essentially the same characteristics for both bands.

The total interband contribution is remarkably flat and the resulting large background which it provides to the total  $\chi(\vec{q})$  would be largely suppressed by the effect of the matrix elements. As no noticeable structure can be observed in the interband part, this contribution will be ignored. The results for  $\chi(\vec{q})$  given in Fig. 2 determined along these several symmetry directions show an absolute maximum to occur at the point R in reciprocal space, which arises essentially from the FS nesting features of the lowest conduction band. Thus, the response function of the conduction electrons of the system shows an instability at the zone boundary R. The Fermi surface can sustain a charge density wave and, even though the phase transition for  $VO_2$  is first order in nature, this instability could manifest itself by an overdamping of the corresponding phonon mode with wavevector  $\vec{q}=(1/2,0,1/2)$ , due to the renormalization of this mode through the electron-phonon coupling. This particular vector is compatible with the change from rutile to monoclinic structure and leads to a doubling of the unit cell in the low temperature phase. To test these predictions, Terauchi and Cohen<sup>20</sup> carried out x-ray diffuse scat-

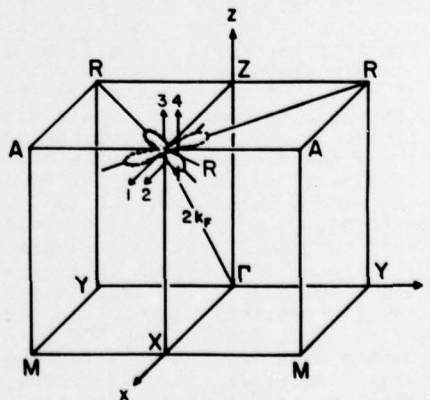


Fig. 3 The Brillouin zone of the rutile phase of  $VO_2$ . The directions employed in measurements near the R-point in Fig. 4 are shown by numbered arrows. Also shown is the diffuse cross of scattering at the R-point expected from a transverse phonon travelling in the R-R direction and polarized in the z direction (after Ref. 20).

tering studies as a function of temperature on VO<sub>2</sub> near the point R(0.5,0,1.5) using CuK<sub>α</sub> radiation. They found that a lattice instability occurs at the R point with wave vector RR and polarization vector parallel to the "c" axis. This result is what is expected if a transverse phonon softens near T<sub>c</sub>, whereas softening of a longitudinal phonon would cause diffuse scattering in the z direction (cf. Fig.3). Their observed diffuse intensity near the R-point at T<sub>c</sub>+3K is shown in Fig.4. Small triangles in the figure give the resolution function estimated from the FWHM of the superlattice reflection (0.5,0,1.5) at T<sub>c</sub>-5K. For the  $\bar{a}^*$  direction through the R-point (see scan 1 in Fig.3) a diffuse intensity maximum is observed at the R-point; however, double maxima are observed for the (0.5+ $\xi$ ,0.08,1.5) direction (scan 2). For the  $\bar{c}^*$  direction there is a single maximum for scan 3, but diffuse scattering could not be detected for run 4. Thus, the x-ray data is consistent with the softening of a transverse phonon near the R-point, as shown in Fig.3.

Terauchi and Cohen<sup>20</sup> also studied the temperature dependence of the diffuse scat-

tering which is expected of a soft phonon. They found the diffuse intensity to increase with decreasing temperature as T approaches T<sub>c</sub>.

#### 4. DISCUSSION

All the results reported here were done in the constant matrix element (ME) approximation to Eq.2. We have discussed the justification for this in detail elsewhere<sup>2</sup>. Basically, in all these cases considered here, the dominant structure arises from the peaks in the intraband part of  $\chi(\vec{q})$ . Using a Wannier function representation, the intraband matrix elements can be shown<sup>2</sup> to modify the constant ME results by a slowly varying function - essentially the square of the form factor. By contrast the interband part of  $\chi(\vec{q})$ , which is large in magnitude and structureless, is zero when ME are included. All previously reported results<sup>21</sup> with ME included show that this "background" contribution is largely suppressed for all  $\vec{q}$  values. Hence we do not expect the interband contribution with ME to give rise to sharp structure nor our general conclusions to be severely affected.

We have presented striking and detailed correlations between our  $\chi(\vec{q})$  results and experiment in a variety of cases. Thus, one must consider the role of the response function as an essential element which must be considered in a more complete microscopic theory which includes many-body effects, local field corrections and electron-phonon matrix elements. Unfortunately, due to the intricacies of the theoretical formulations proposed to date, accurate and reliable ab initio calculations are not yet feasible. Hence, one must be concerned with approximations made in any of these attempts. What is clear from our studies is the importance of including structure of the diagonal elements of the susceptibility matrix in any theoretical formulation.

#### ACKNOWLEDGEMENTS

One of us (AJF) is grateful to J.B. Cohen for discussions of his x-ray studies and for permission to reproduce Figs. 3 and 4. This paper was written by one of us (AJF) while at the Technische Universität München as an Alexander von Humboldt Stiftung Senior Fellow; the hospitality of Profs. G.M. Kalvins and R.L. Mössbauer and their colleagues and the support of the Alexander von Humboldt Stiftung is gratefully acknowledged.

#### REFERENCES

1. MYRON, H., RATH, J., and FREEMAN, A.J., Phys. Rev. B **15**, 885 (1977).
2. GUPTA, M. and FREEMAN, A.J., Phys. Rev. B **14**, 5205 (1976).
3. WATSON-YANG, T.J. and FREEMAN, A.J., Bull. Am. Phys. Soc. **22**, 103 (1977) and to be published.
4. FREEMAN, A.J., GUPTA, M., and ELLIS, D.E., Bull. Am. Phys. Soc. **22**, 474 (1977) and Phys. Rev. (to appear).

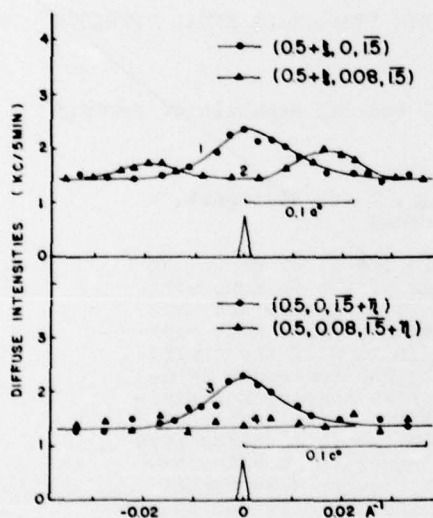


Fig.4 The diffuse intensities for the 4 directions given in Fig.3 near the R-point at T<sub>c</sub>+3K. Small triangles show the FWHM of the superlattice reflection (0.5,0,1.5) at T<sub>c</sub>-5K (after Ref.20).

5. RATH, J. and FREEMAN, A.J., Phys. Rev. B 11, 2109 (1975). The same formulae were derived independently by LINDGARD, P.A., Sol. St. Comm. 16, 481 (1975).
6. JEPSEN, O. and ANDERSEN, O.K., Sol. St. Comm. 9, 1763 (1971).
7. LEHMAN, G. and TAUT, M. Phys. Stat. Solidi 54, 469 (1972).
8. WILSON, J.A., DISALVO, F.J., and MAHAJAN, S., Phys. Rev. Lett. 32, 882 (1974); Adv. Phys. 24, 117 (1975).
9. WILLIAMS, F.M., FARRY, G.S., and SCRUBY, C.B., Philos. Mag. 29, 695 (1974).
10. MATTHEISS, L.F., Phys. Rev. B 8, 3719 (1973).
11. ZUNGER, A. and FREEMAN, A.J., Phys. Rev. (to be published).
12. SMITH, H.G. and GLÄSER, W., Phys. Rev. Lett. 25, 1611 (1970); SMITH, H.G., in "Superconductivity in d and f Band Metals", ed. by D.H. Douglass (AIP, New York, 1972).
13. WEBER, W., Phys. Rev. B 8, 5082 (1973).
14. MILLER, A.P. and BROCKHOUSE, B.N., Can. J. Phys. 49, 704 (1971).
15. DUTTON, D.H., BROCKHOUSE, B.N., and MILLER, A.P., Can. J. Phys. 50, 2915 (1972).
16. MILLER, A.P., Can. J. Phys. 53, 2491 (1975).
17. WATSON-YANG, T.J., HARMON, B.N., and FREEMAN, A.J., J. Mag. and Magn. Mat'ls 2, 334 (1976).
18. FRADIN, F.Y., KOELLING, D.D., FREEMAN, A.J., and WATSON-YANG, T.J., Phys. Rev. B 12, 5570 (1975).
19. WATSON-YANG, T.J. and FREEMAN, A.J., (to be published).
20. TERAUCHI, H. and COHEN, J.B., (to be published).
21. GUPTA, R.P. and SINHA, S.K., Phys. Rev. B 3, 2401 (1971); COOKE, J.F., DAVIS, H.L., and MOSTOLLER, M., Phys. Rev. B 9, 2485 (1974); GUPTA, R.P. and FREEMAN, A.J., Phys. Rev. B 13, 4376 (1976).

LATTICE SPECIFIC HEAT AND PHONON ANOMALIES IN CUBIC TRANSITION METAL NITRIDES

F. Roedhammer

Fachbereich Physik, Universität, D-7750 Konstanz, Federal Republic of Germany

E. Gmelin

Max-Planck-Institut für Festkörperforschung, D-700 Stuttgart,  
Federal Republic of Germany

The mononitrides of the transition metals (TM's) of group IVb have physical properties similar to those of the Vb monocarbides. They also crystallize in the rocksalt structure and have high melting points; they are also superconducting, with transition temperatures between 5K and 10K. In view of the empirical correlation between superconductivity and soft-mode behavior in the Vb carbides it is of interest whether or not similar phonon anomalies exist in the IVb nitrides. We have shown previously<sup>1</sup> that the phonon anomalies in the Vb carbides give rise to an excess specific heat at low temperatures with respect to the "normal" IVb carbides. In this paper<sup>2</sup> we report on measurements of the specific heat of the IVb nitrides at low temperatures ( $1.5 < T < 90\text{K}$ ). We have detected an excess term in the lattice specific heat at low temperatures of the IVb nitrides from a comparison with the lattice specific heat of the corresponding IVb carbides. Since the limiting value of the Debye temperature  $\theta_D$  ( $T \rightarrow 0$ ) is approximately constant for the nitride and the carbide of a given IVb TM we attribute this excess term to the evolution of a soft-mode region in the acoustic part of the phonon dispersion of the nitride. An analysis based on the Einstein model yields the onset (i.e. the lowest) frequency  $\nu_E$  of the soft-regime: 5.8 THz for TiN<sup>3</sup>, 4.5 THz for ZrN and 2.8 THz for HfN. These onset frequencies agree very well with each other and with the corresponding values for the Vb carbides if they are appropriately scaled with the respective mass of the TM atom. This indicates that the mechanism which drives the phonon anomalies is closely related in all these compounds. By analogy to the Vb carbides  $\nu_E$  would then represent the transverse acoustic phonon frequency at the L point.